ELSEVIER

Journal of Pharmaceutical and Biomedical Analysis
19 (1999) 153–161

JOURNAL OF
PHARMACEUTICAL
AND BIOMEDICAL
ANALYSIS

Feasibility studies of simultaneous multianalyte amperometric immunoassay based on spatial resolution

Ying Ding, Liping Zhou, H. Brian Halsall *, William R. Heineman

Department of Chemistry, University of Cincinnati, PO Box 210172, Cincinnati, OH 45221-0172, USA

Received 21 March 1998; accepted 16 July 1998

Abstract

A multianalyte immunoassay concept based on the geometric separation of different analyte-specific antibodies has been demonstrated. The assay and amperometric detection are done in a cell with two working electrodes controlled at the same potential, and the amperometric signal at each electrode is monitored. The distance between any two adjacent electrodes in this prototype is 2.5 mm, and during the course of amperometric measurement, the product formed at one electrode does not reach the other working electrode within 20 min after the addition of enzyme substrate. Thus, the method relies on the spatial resolution between the different antibodies being such that measurements are taken before cross-interference due to diffusion can occur. Identical enzyme labels (alkaline phosphatase, ALP) and substrates (*p*-aminophenyl phosphate, PAPP) are used for all analytes. Alkaline phosphatase-conjugated rat anti-mouse IgG was immobilized by passive adsorption. Our studies showed that this concept is feasible and can be applied to the simultaneous measurement of multiple analytes.

Keywords: Analyte-specific antibodies; Amperometric detection; Multianalyte immunoassay; Spatial resolution

1. Introduction

Simultaneous multianalyte immunoassay (SMIA), in which two or more analytes are measured simultaneously in a single assay, represents the next major advance in immunoassay methodology [1]. SMIA is important because it uses less sample, the test throughput is increased, and the overall cost per test is decreased. The first SMIA, in which human insulin and growth hormone in serum were measured using two different radioisotope labels, I-131 and I-125, was reported in 1966 [2]. Since then, various approaches for SMIA have been demonstrated [3]. Many of these involve the use of multiple labels, such as radioisotopes [4–8], DNA [9] and fluorophores [10,11]. Other ways of performing SMIA include a microspot assay [12], a method based on spatially distinct fluorescent areas quantitated by laser-excited solid-phase time-resolved fluorometry [13], and a nonseparation electrochemical enzyme immunoassay using multiple gold films deposited on the same membrane [14].

* Corresponding author. Tel.: +1 5569210; fax: +1 513 5569239; e-mail: brian.halsall@uc.edu

0731-7085/99/$ - see front matter
PII S0731-7085(98)00186-1

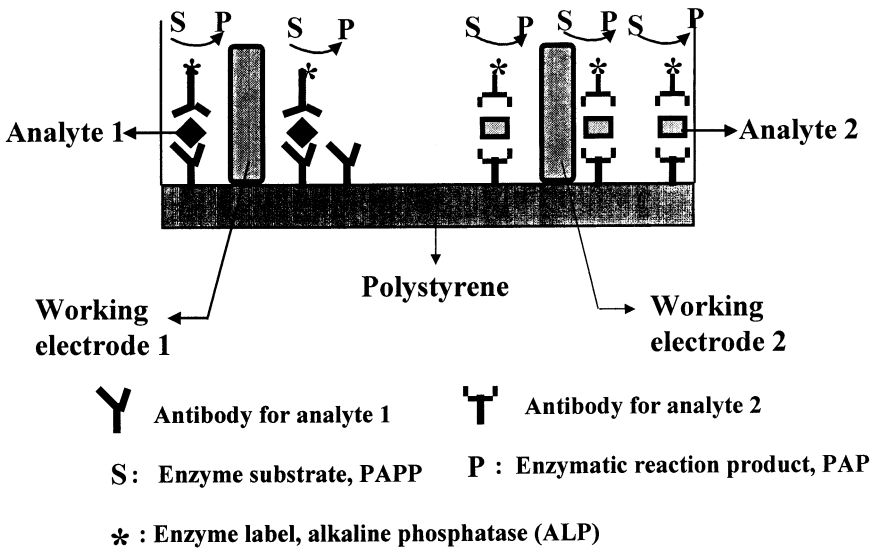

Fig. 1. Multianalyte immunoassay based on spatial resolution (sandwich format). In the work described here, analytes 1, 2 and analyte antibodies 1, 2 are omitted, the labeled antibody being attached directly to the polystyrene.

Electrochemistry is one of the most sensitive analytical methods, and has been shown to be an effective technique for detection in immunoassay [15–26]. The assay is based on labels that are either electroactive or catalyze the production of an electroactive product [15]. Electrochemical immunoassay has many features in common with other types of immunoassay and one that is less well shared, but very important, in that it can be miniaturized easily. This is especially important in the development of disposable devices and methodology for ultra-small sample amounts. The potential exists for development of simple electrochemical immunoassay kits for applications that require small, portable systems.

We previously reported the development of a simultaneous dual-analyte immunoassay method based on releasable metal ion labels, and we demonstrated its potential for use in the clinical laboratory [27]. That approach, however, was not generic due to the fact that a different metal label is needed for each analyte, and the detection limit was higher than with enzyme labels. The focus of our recent SMIA strategy has been on simplification and making the assay more generic. The concept we are now developing is based on the separation between different analyte-specific antibodies, i.e. different antibodies are immobilized at distinct areas on a solid phase. After analytes are bound, enzyme-labeled antibodies or antigens, depending on the assay format used (sandwich or competitive), are added and bind to their respective analyte specific region. The amount of enzyme reaction product generated at each area is quantitated by simultaneous amperometric measurements at an independent microelectrode for each area. This method relies on the spatial resolution between the different antibodies and the requirement that measurements be taken before cross-interference due to diffusion of product can occur. These concepts are illustrated in Fig. 1, using the sandwich immunoassay format.

Methods for SMIA that combine two or more enzyme labels involve a compromise in the final assay conditions because different enzymes have different requirements or optimum enzyme activities [28]. In our method, the same enzyme label (alkaline phosphatase, ALP) and substrate (*p*-aminophenyl phosphate, PAPP) are used for each analyte. *p*-Aminophenol (PAP) is produced from PAPP by ALP and is then measured by amperometric oxidation as described by the following reactions [16]:

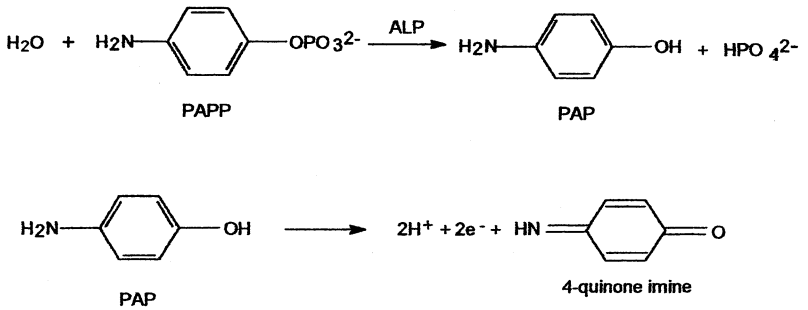

Since the same enzyme product, PAP, is generated around each working electrode, measurements must be taken at each area before cross-interference due to PAP diffusion can occur. This method therefore relies on there being a minimum distance between the enzyme-labeled moieties. In the work described here we simulate this concept by taking the passive adsorption of enzyme labeled antibody (Ab*) to polystyrene as being equivalent to the binding of Ab* to captured analyte in an immunoassay. This is done merely as a convenience to locate Ab* in specific regions of the electrochemical cell.

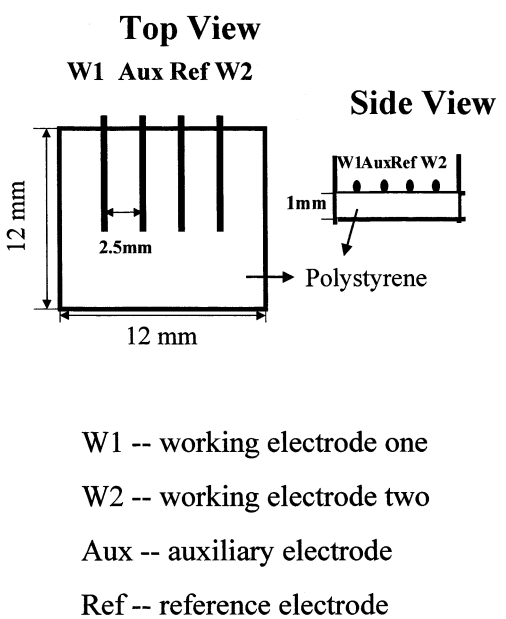

Fig. 2. Schematic diagrams of the dual working electrode cell.

2. Experimental section

2.1. Device fabrication

A macroscopic prototype dual working electrode cell was fabricated to study the fundamental aspects of this method and evaluate the concept. The cell was made of teflon, and its design is illustrated in Fig. 2. It consists of two gold wire (0.25 mm diameter, 99.99%, from Aldrich) working electrodes, one silver-silver chloride wire reference electrode and one platinum wire (0.25 mm diameter, 99.9%, from Aldrich) auxiliary electrode. Silver wire was from BAS (Bioanalytical Systems, West Lafayette, IN) and silver chloride was electrolytically deposited on it by anodization in 0.1 M HCl. Both working electrodes share the reference and auxiliary electrodes. These four electrodes were inserted into the side holes of the cell before each assay. Antibody (in this case Ab*) is immobilized on a piece of polystyrene sheet attached to the bottom of the cell. The electrodes rest on the polystyrene surface, leaving no gap in-between. The distance between any two adjacent electrodes is 2.5 mm. Both the assay and electrochemical detection were carried out in this cell, which had a volume of 150 μl with the polystyrene base present and 300 μl without it.

2.2. Materials and reagents

Alkaline phosphatase-conjugated affinipure rat anti-mouse IgG (Ab*; H + L) was obtained from Jackson Immunoresearch Laboratory (West Grove, PA). Tris (hydroxymethyl) aminomethane and *p*-aminophenol (98%) were obtained from Aldrich (Milwaukee, WI). *p*-Aminophenyl phos-

phate was synthesized as previously reported [16]. Polystyrene sheet (white, opaque, thickness 0.03 in) was from Cincinnati Plastics (Cincinnati, OH).

2.3. Buffers and solutions

(a) Tris buffer: 0.1M tris (hydroxymethyl) aminomethane, 1 g ml^{-1} magnesium chloride, and 0.01% (w/v) sodium azide, adjusted to pH 9.0 with hydrochloric acid; (b) acetate buffer: 0.1M sodium acetate-acetic acid, pH 5; (c) Ab* solution: 1:10000 or 1:20000 dilution from Ab* stock solution (0.45mg ml^{-}) with acetate buffer; (d) substrate solution: 4mM PAPP in 0.1M tris buffer; (e) PAP solutions were made in 0.1M tris buffer. All solutions were made with doubly-deionized water from a Barnstead (Boston, MA) Nanopure/Organicpure water system.

2.4. Apparatus

A 179 TRMS digital multimeter was used to measure the reference electrode's potential (Keithly Instruments, Cleveland, OH). A dual-potentiostat system was set up by connecting two BAS LC-4C detectors (Bioanalytical Systems, West Lafayette, IN) together. Each LC-4C controls the potential and measures the current of its assigned working electrode independently. The current signals were recorded by a strip chart recorder (Fisher Recordall, Series 5000, Pittsburgh, PA).

2.5. Cell preparation

A piece of polystyrene (12 mm × 12 mm) was attached to the bottom of the cell with double-sided tape. The cell was washed with methanol and then water. After the electrodes were slid into the cell, they were cleaned electrochemically (+ 1000 mV for 5 s, − 600 mV for 25 s and + 600 mV for 10 s).

2.6. Analysis procedure

Two hundred μl of Ab* solution were pipetted into the cell (filling the cell above the electrodes), incubated for 12 h at 4°C, and removed by aspiration. After rinsing with tris three times, 200 μl of PAPP solution were added to the cell, and the enzymatic reaction was allowed to proceed in the dark for 20 min. For blank experiments, the acetate buffer with no Ab* was incubated for 12 h, and then the same procedure was followed. No attempt has been made here to present an optimal preparation procedure in terms of incubation time and solution composition.

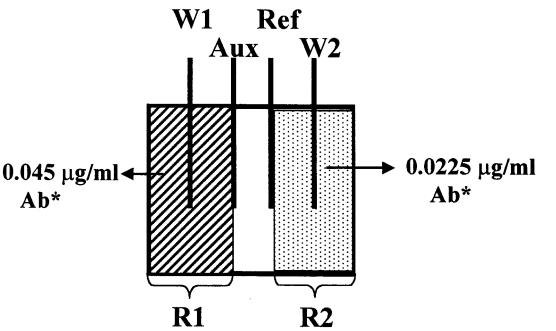

Fig. 3. Schematic for dual analyte immobilization. W_1, working electrode one; W_2, working electrode 2; Aux, auxiliary electrode; Ref, reference electrode; Ab*, enzyme-labeled antibody.

2.7. Electrochemical measurements

The dual-potentiostat was turned on to record the current signals every 2 or 5 min after substrate addition for a total time of 20 min. Both working electrodes were held at + 300mV vs the reference electrode. At 10 s after turning on the dual-potentiostat, the current signals at the two working electrodes were recorded. The dual-potentiostat was then turned off until the next measurement was to be made.

2.8. Simultaneous dual assay experiment

After a freshly-cut polystyrene piece was fixed in the cell, 50 μl Ab* (0.045 μg ml^{-}) were pipetted into region one (R_1), covering the area from the auxiliary electrode to the left side of the cell-wall. The auxiliary electrode acted as a barrier to prevent solution from leaking away to other areas. Another 50 μl of 0.0225 μg ml^{-} conjugate were pipetted into region two (R_2), covering the area from the reference electrode to the right side of the cell-wall. The reference electrode acted as a

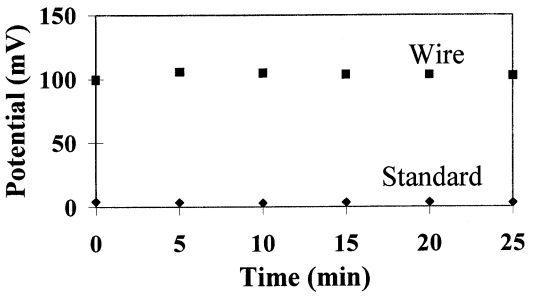

Fig. 4. Potential stability study of wire reference electrode. Each electrode potential was measured versus a saturated calomel electrode (SCE) in 5 μM PAP, Tris buffer solution.

barrier at the right side (Fig. 3). The solution connection of the cell is provided by the addition of 200 μl PAPP solution during the detection step. The incubation step and detection procedures were the same as stated above.

3. Results and discussion

3.1. Potential stability of wire reference electrode

Our first concern in this study was the stability of the Ag/AgCl wire reference electrode half-cell potential. Since it is not isolated in a solution of constant Cl^- activity, which is the case for standard Ag/AgCl reference electrodes, the stability of its potential during the course of the electrochemical measurements is an important factor in determining the accuracy of the measurements. Furthermore, the electrode is exposed to the chemicals in the immunoassay procedure, including the reducing agent PAP in the final assay detection step, and this might also affect the potential of the bare Ag/AgCl electrode causing a shift in the optimum detection potential. The stability of the reference electrode was evaluated by immersing the Ag/AgCl wire in tris buffer and measuring its potential versus a commercial saturated calomel electrode (SCE). A plot of the potential difference between the wire reference electrode and the SCE vs time (Fig. 4, wire) shows a stable potential (within 6 mV) for 25 min, which is the time for an assay. This stability is compared to that of a commercial Ag/AgCl reference electrode, for which the Ag/AgCl wire is immersed in 3 M NaCl (Fig. 4, standard vs. SCE in the same buffer solution). The + 100 mV potential difference between the bare wire reference electrode and the commercial Ag/AgCl reference electrode is due to the different Cl^- activities contacting the Ag/AgCl wire ($[Cl^-]_{wire} = 9.84$ mM), and the commercial Ag/AgCl reference electrode ($[Cl^-]_{standard} = 3.00$M). The calculated potential difference would be about 147 mV assuming room temperature and equivalence of the Cl^- activity and the Cl^- concentration. As long as the wire reference electrode potential stays constant during the enzyme reaction stage, which in our study is 20 min, the amperometric measurements taken at the end of the reaction are free from possible errors due to shifts in the reference electrode half-cell potential.

3.2. Cross-interference study

Since this method is based on the continuing resolution of the PAP generated for each analyte, measurement has to be taken before cross-interference due to PAP diffusion to the working electrode for the other analyte can occur. The Einstein equation can be used to calculate the distances molecules move by diffusion. Fig. 5 shows a calculated distance-time plot for a diffusion coefficient (D) of 10^{-5} cm^2 sec^{-1}, giving an upper limit of the distance that PAP molecules on the average can travel in a quiescent solution[29]. In 20 min, PAP molecules would travel a maximum of 1.5 mm. The electrodes in our cell and

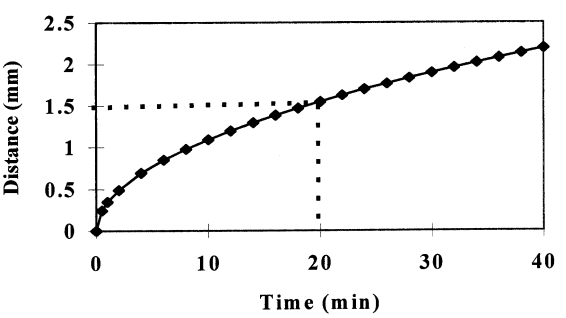

Fig. 5. Diffusion profile of PAP. The curve is plotted according to the Einstein equation: $d = \sqrt{2Dt}$, d is the distance that PAP molecules will move on the average, cm; D is diffusion coefficient, cm^2 sec^{-1}; t is time, sec.

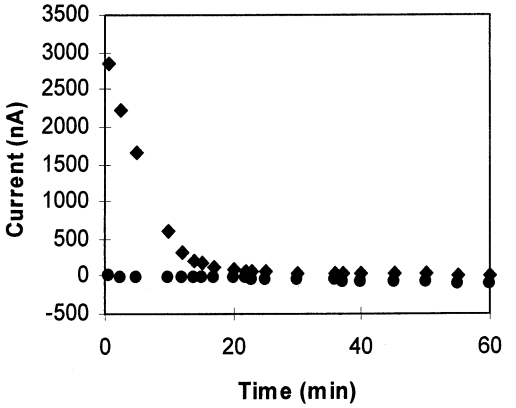

Fig. 6. PAP diffusion experiment. W_1 was held at +300 mv, W_2 was held at −200 mv. 5 μM PAP was in the cell. ◆ represents oxidation current, ■ represents reduction current.

the edges of the Ab immobilization regions were 2.5 mm apart, which should be enough to avoid cross-interference.

A PAP diffusion experiment was conducted to test this conclusion (Fig. 6). A solution of PAP was added to the cell, W_1 was held at +300 mV so that PAP was oxidized under diffusion-controlled conditions, and W_2 was held at −200 mV, at which potential oxidized PAP would be reduced. PAP oxidized at W_1 would diffuse away, and its arrival at W_2 would be signaled by an increase in reduction current. As shown in the plot, there was no noticeable increase in reduction current within 60 min, indicating that oxidized PAP had not yet diffused to W_2 in detectable quantity. Therefore, during the course of amperometric measurement, the product formed at one electrode has not reached the other working electrode 20 min after the addition of enzyme substrate, and our measurements can be cross-interference-free.

3.3. Quantitation of PAP

Chronoamperometry was used to detect enzyme-generated PAP. Other techniques could be used as well, but due to the convenience and availability of the BAS dual-potentiostat, chronoamperometry was used here. In this method, the current measured is a function of

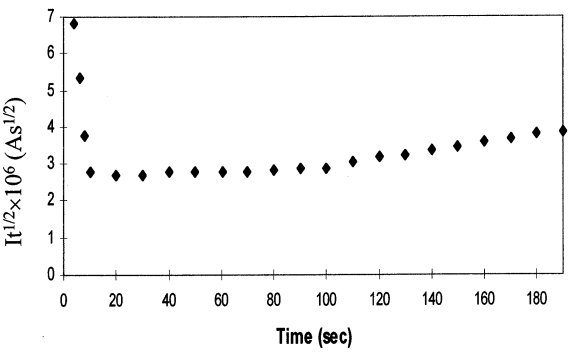

Fig. 7. Cottrell plot for the system. 50 μM PAP was in the cell. The filters of the dual-potentiostat were set at 0.1 Hz.

time, the concentration of electrochemically active species and other factors. These are embodied in the Cottrell equation:

$$i_t = \frac{nFAC^0\sqrt{D}}{\sqrt{\pi t}}$$

where i_t = current at time t, amperes; D = diffusion coefficient, $cm^2\ s^{-1}$; A = electrode area, cm^2; F = Faraday's constant, 96485 C eq^{-1}; C^0 = concentration at electrode surface, mol cm^{-3}, t = time, sec. If t is fixed, i_t varies linearly with C^0. Although this equation is for a planar electrode, nonplanar electrodes such as the wire electrode used in this method will obey it at sufficiently short times since the curvature of the electrode

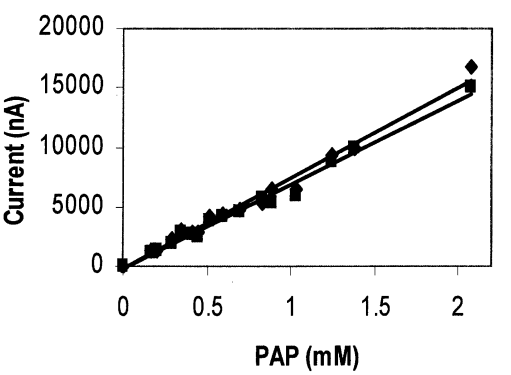

Fig. 8. The current–concentration plot for PAP using chronoamperometry with readings taken at $t = 10$ s. ◆ represents the current signal at W_1 (i_1), ■ represents the current signal at W_2 (i_2). The line for i_1 follows $y = 7.68 \times 10^3 \times -270$. The line for i_2 follows $y = 7.10 \times 10^3 \times -197$.

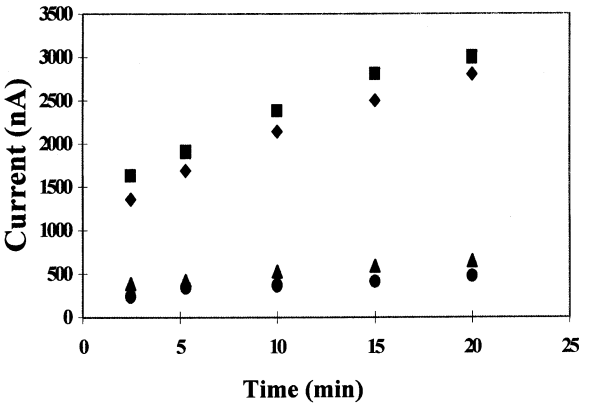

Fig. 9. Response time curves for rat anti-mouse IgG ALP conjugate. ■ and ◆ are i_1 and i_2 for Ab* concentration of 0.045 μg ml^{-1}. ▲ and ● are blank signals.

surface is then negligible relative to the depth of the diffusion layer [30]. Fig. 7 is a Cottrell plot ($it^{1/2}$ vs t) for this electrochemical detection system. Under the experimental conditions, the available time window during which $it^{1/2}$ is a constant with respect to t for Cottrell measurements of this system is between 8 and 100 s. The large positive deviation of $it^{1/2}$ at $t < 8$ s is likely due to the slow charging of the electrode double layer during the potential step. The positive deviation at $t > 100$ s can be a result of nonplanar diffusion and/or convection in the cell. The current signals taken in this time window will have a linear relationship with the concentration of electroactive species. The earlier the measurements are taken, the larger the current signals, and therefore, the more sensitivity the detection will have.

Fig. 8 shows current–concentration plots for PAP at both working electrodes using this method with the current measured at 10 s. A slight difference between the two working electrodes is evidenced by the curves in the concentration range of 0–2 mM.

3.4. Simultaneous detection of dual analytes

The concept of the spatial resolution dual immunoassay is based on being able to do separate immunoassays in the two regions (R_1, R_2) of the electrochemical cell. This was evaluated with three types of experiments.

1. We established that Ab* could be passively immobilized on polystyrene. Identical concentrations of the same Ab* were immobilized in the two regions (R_1, R_2). Substrate was then added and the signals at W_1 and W_2 were recorded. As shown in Fig. 9, the detection signals at both W_1 and W_2 increase with time as PAP concentrations increase in each region, which is the expected result if Ab* has been immobilized. Although the same procedure was carried out in both regions of the cell, the currents are not identical at both electrodes. The difference is attributed to differences in electrode surface area, inexact positioning of W_1 and W_2 with respect to the polystyrene surface, and different amounts of Ab* being immobilized in the two regions. These variables are all difficult to control with the prototype cell, but this can be overcome with a different cell fabrication strategy (vide infra). The blank also gave a slight increase in signal from non-enzymatic PAPP hydrolysis.
2. We were able to detect independently different concentrations of enzyme label in the two regions (Fig. 10). A volume of 0.045 μg ml^{-1} of Ab* was immobilized around W_1, and 0.0225 μg ml^{-1} of Ab* around W_2 (Fig. 3). Since the concentration of Ab* at W_1 was

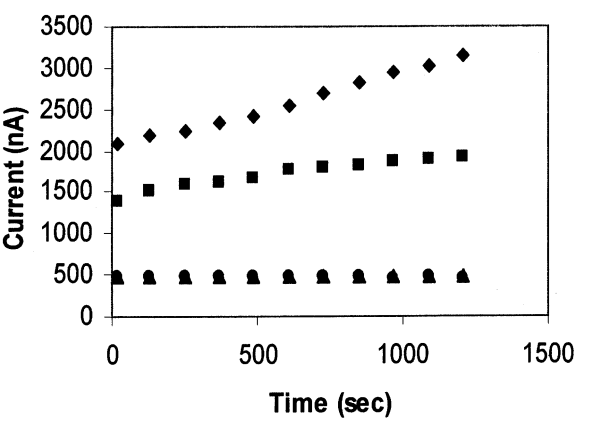

Fig. 10. Response time curves for simultaneous detection of two different concentrations of antibody conjugates. ◆ and ■ represent signals obtained for Ab* concentration of 0.045 μg ml^{-1} and 0.0225 μg ml^{-1} respectively, with slopes of 0.90 nA sec^{-1} and 0.43 nA sec^{-1}, respectively. ● and ▲ are blank signals.

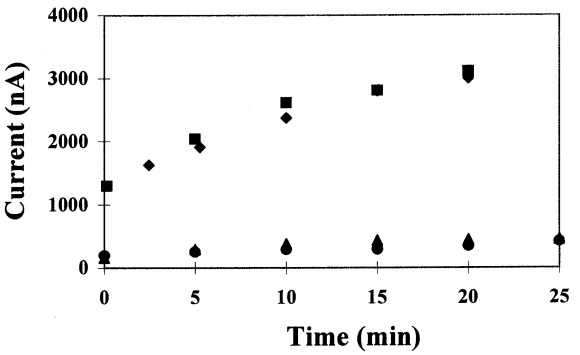

Fig. 11. Cross-interference study of simulated assays systems. ◆ represents the current signals obtained for Ab_1^* in a single 'analyte assay, ■ represents those obtained for Ab_1^*' in a simultaneous 'dual analyte assay', configured as in Fig. 3, ▲ represents those obtained for Ab_2^* in a 'single analyte assay', ● represents those obtained for Ab_2^* in a simultaneous 'dual analyte assay', configured as in Fig. 3.

twice that at W_2, it was expected that the enzymatic reaction rate at W_1 would be twice that at W_2, and that the di_1/dt would also be twice that of i_2. This is what was found from the graph as an expected slope ratio of two, and so we conclude that the signals associated with each individual zone can be quantitated simultaneously.

3. We showed that 'cross-talk' between the two regions could be avoided. Fig. 11 shows that the presence or absence of one concentration of Ab* (designated Ab_1^*) in one region does not affect the amperometric signal observed at the individual working electrode for a different concentration of Ab* (designated Ab_2^*) in the second region. ◆ represents the current signals obtained at W_1 when only Ab_1^* was immobilized in the entire cell (i.e. they mimic the signals for Ab_1^* from a single analyte assay). ■ represents the current signals obtained with Ab_1^* immobilized at W_1 and Ab_2^* at W_2. These mimic the signals for Ab_1^* from a simultaneous dual analyte assay. These two sets of data agree very well with each other. The same result was obtained for Ab_2^*, as shown by the congruency of the ▲ and ● symbols. Since the method can measure two concentrations of antibody conjugate in the presence of each other without interference, the concept of multianalyte electrochemical immunoassay based on spatial resolution is therefore feasible and can be applied to the simultaneous measurements of multiple analytes.
4. Finally, we calculated the concentrations of PAP generated at the two working electrodes during the experiment for Fig. 10 according to the calibration curves (Fig. 8). The slope ratio between the two lines is also very close to two (Fig. 12).

4. Conclusions

Spatial resolution of immobilized antibody combined with amperometric detection is the strategy adopted here. By localizing the different analyte-specific antibodies in different regions, analytes are separated spatially. The closely spaced areas, each of which represents one analyte, are individually quantitated by microelectrodes in those areas. In theory an unlimited number of analytes can be assayed by this principle. In this paper, this principle has been demonstrated using a dual system. To explore the many possibilities of electrochemical detection, we are applying micromachining technology to this multianalyte immunoassay study. We are in the process of

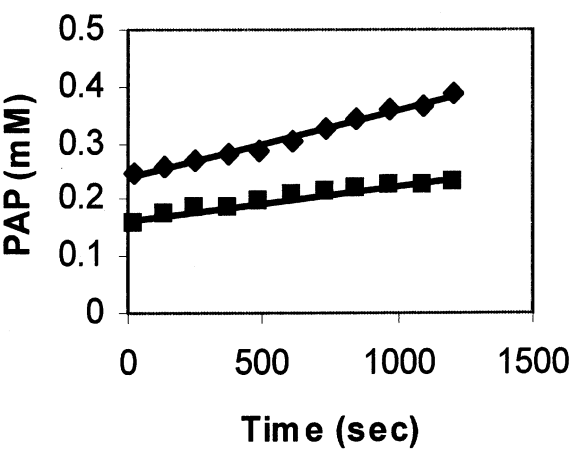

Fig. 12. The concentration of PAP generated at different times at different working electrodes. ◆ represents the concentration of PAP generated at working electrode 1, ■ represents the concentration of PAP generated at working electrode 2.

developing a micro-electro-mechanical systems (MEMS) device, which in this case will be a thumb-nail-size or smaller chip cell and we anticipate that this will provide SMIA with more versatility as a sensitive, economic and practical approach. For three or more analytes, it will require three or more immobilization regions and detecting electrodes, which will simply mean that one or more metal strips must be deposited to add one or more working electrodes to the electrochemical cell. We anticipate that this combination of electrochemical detection coupled with innovative assay design and micromachining technology will lead to a more efficient and practical multianalyte immunoassay.

References

[1] R. Ekins, F. Chu, Clin. Chem. 39 (2) (1993) 369–370.
[2] C. Morgan, R. Proc. Soc. Exp. Biol. Med. 123 (1966) 230.
[3] L.J. Kricka, in: E.P. Diamandis, T.K. Christopoulos (Eds.), Immunoassay, Academic Press, New York, 1996, pp. 389–404.
[4] S. Gutcho, L. Mansbach, Clin. Chem. 23 (9) (1977) 1609–1614.
[5] F.H. Wians, J. Dev, M.M. Powell, J.I. Heald, Clin. Chem. 32 (1986) 887–890.
[6] T. Mitsuma, J. Colucci, L. Shenkman, C.S. Hollander, Biochem. Biophys. Res. Commun. 45 (1972) 2113.
[7] J.G. Ljunggren, B. Persson, M. Tryselius, Acta Endocrinol. 81 (1976) 487–494.
[8] S.P. Haynes, D.J. Goldie, Ann. Clin. Biochem. 14 (1977) 12–15.
[9] E.R. Hendrickson, T.M. Hatfield Truby, R.D. Joerger, W.R. Majarian, R.C. Ebersole, Nucleic Acids Res. 23 (3) (1995) 522–529.
[10] I. Hemmila, S. Holttinen, K. Petterson, T. Lovgren, Clin. Chem. 33 (1987) 2281–2293.
[11] M. Saarma, L. Jarvekulf, I. Hemmila, H. Siitari, R. Sinijarv, J. Virol. Method. 23 (1989) 47–54.
[12] R.P. Ekins, F.W. Chu, Clin. Chem. 37/11 (1991) 1955–1967.
[13] S.E. Kakabakos, T.K. Christopoulos, E.P. Diamandis, Clin. Chem. 38/3 (1992) 338–342.
[14] M.E. Meyerhoff, C. Duan, M. Meusel, Clin. Chem. 41/9 (1995) 1378–1384.
[15] W.R. Heineman, H.B. Halsall, Anal. Chem. 57 (1985) 1321A–1331.
[16] H.T. Tang, C.E. Lunte, H.B. Halsall, W.R. Heineman, Anal. Chim. Acta. 214 (1988) 187–195.
[17] S.H. Jenkins, W.R. Heineman, H.B. Halsall, Anal. Biochem. 168 (1988) 292–299.
[18] Y. Xu, H.B. Halsall, W.R. Heineman, J. Pharm. Biomed. Anal. 7/12 (1989) 1301–1311.
[19] Y. Xu, H.B. Halsall, W.R. Heineman, Clin. Chem. 36 (11) (1990) 1941–1944.
[20] E.P. Gil, H.T. Tang, H.B. Halsall, W.R. Heineman, A.S. Misiego, Clin. Chem. 36 (4) (1990) 662–665.
[21] Y. Xu, H.B. Halsall, W.R. Heineman, in: R. Nakamura, Y. Kasahara, G. Rechnitz (eds.), Immunochemical Assays and Biosensor Technology for the 1990's, American Society Microbiology Press, New York, 1992, pp. 291–309.
[22] H. Yao, S.H. Jenkins, A.J. Pesce, H.B. Halsall, W.R. Heineman, Clin. Chem. 39 (7) (1993) 1432–1434.
[23] O. Niwa, Y. Xu, H.B. Halsall, W.R. Heineman, Anal. Chem. 65 (1993) 1559–1563.
[24] N. Kaneki, Y. Xu, A. Kumari, H.B. Halsall, W.R. Heineman, Anal. Chim. Acta. 287 (1994) 253–258.
[25] H. Yao, H.B. Halsall, W.R. Heineman, S.H. Jenkins, Clin. Chem. 41 (4) (1995) 591–598.
[26] C.G. Bauer, A.V. Eremenko, E. Ehrentreich-Förster, F.F. Bier, A. Makower, H.B. Halsall, W.R. Heineman, F.W. Scheller, Anal. Chem. 68 (15) (1996) 2453–2458.
[27] F.J. Hayes, H.B. Halsall, W.R. Heineman, Anal. Chem. 66 (11) (1994) 1860–1865.
[28] L.J. Kricka, Clin. Chem. 38 (3) (1992) 327–328.
[29] A.J. Bard, L.R. Faulkner, Electrochemical Methods: Fundamental and Applications, Wiley, New York, 1980, pp. 128–129.
[30] P.T. Kissinger, W.R. Heineman (Eds.), Laboratory Techniques in Electroanalytical Chemistry, 2nd ed., Marcel Dekker, New York, 1996, pp. 55–60.